

PACS numbers: 42.55.Px; 78.20.Jq; 42.79.Hp
DOI: 10.1070/QE2007v037n07ABEH013495

Multichannel optical modulator for a laser diode array

S.I. Derzhavin, V.V. Kuz'minov, D.A. Mashkovskii, V.N. Timoshkin

***Abstract*. The possibility of the development of a multichannel electrooptical modulator of laser radiation with a large diffraction divergence and a small coherence length is studied experimentally and its design is described.**

Keywords: *laser diode array, electrooptical modulator, quality parameter, diffraction divergence.*

1. Choice of the modulator scheme and material

The development of new optical schemes for recording and reading large information volumes requires the fabrication of multichannel optical modulators. To make these devices miniature, diode lasers are used. However, the radiation of these lasers has a large diffraction divergence, which strongly complicates the operation of the optical modulator. In this paper, we solve the problem of a large divergence and a small coherence length of diode lasers used in electrooptical modulators.

Electrooptical modulators can be based on the known crystals such as KDP, ADP, GaAs, ZnS, ZnTe, $LiNbO_3$, $LiTaO_3$, and $BaTiO_3$. The choice of one or another crystal for using in a modulator depends on its symmetry group, which determines the properties of the crystal. The choice of an appropriate crystal in our work was based on the following requirements:

(i) the possibility of the modulator to operate with radiation at a wavelength of 0.8 μm with the spectral width $\Delta\lambda = 3$ nm (typical for high-power laser diode arrays);

(ii) the minimisation of the operating voltage ($V <$ 350 V);

(iii) the modulation efficiency at low frequencies (to 100 kHz);

(iv) the minimisation of the destructive role of effects accompanying a high density of channels, a high output power (up to 100 mW per channel) and the beam quality factor $M^2 = 5$ for the modulation depth no worse than 90 %;

(v) the absence of necessity in thermal stabilisation (which simplifies the modulator design due the absence of a heat exchanger);

(vi) the possibility of making a miniature modulator (which also includes the removal of restrictions on the cost of materials).

Our analysis of various crystals and modulator schemes has shown that most of the crystals mentioned above do not satisfy these requirements. Thus, the KDP and ADP crystals (the symmetry group $\bar{4}2m$) can operate only with highly monochromatic radiation with the spectral width $\Delta\lambda$ determined by the relation [1]

$$\frac{\Delta\lambda}{\lambda} \leqslant \frac{\lambda}{4(n_e - n_o)L}, \qquad (1)$$

where λ is the radiation wavelength; n_o and n_e are the refractive indices for the ordinary and extraordinary waves, respectively; and L is the crystal length. The radiation linewidth of a source for these crystals of typical length $L = 10$ mm should be a few angstroms, which is an order of magnitude smaller than the linewidth of a laser diode array. In addition, the dependences of the refractive indices of the ordinary and extraordinary waves on temperature require the thermal stabilisation of these crystals because the temperature change ΔT only by 0.01 °C produces the additional phase difference of 23° [1]. Although this destructive effect can be removed by using two crystals in tandem by choosing appropriately the modulating-voltage polarity, this complicates the modulator design.

The cubic GaAs, ZnS, and ZnTe crystals (the symmetry group $\bar{4}3m$) have a number of advantages compared to the KDP and ADP crystals, which is related to the absence of natural birefringence in cubic crystals. This circumstance permits the use of cubic crystals in modulators with the angular aperture of 10° and more and also to reduce requirements to the radiation monochromaticity and the temperature stabilisation of the modulator upon using the transverse electrooptical effect [1]. However, the application of these crystals is restricted by difficulties of fabricating high-quality large samples. Nevertheless, GaAs crystals are used in modulators operating in the wavelength range from 0.8 to 16 μm.

A $BaTiO_3$ crystal (the symmetry group $4mm$) of optical quality has a high electrooptical constant; however, it is expensive and, as far as we known, is not manufactured in Russia at present.

As a result, we have chosen a modulator based on a $LiNbO_3$ crystal (the symmetry group $3m$) operating by using the transverse linear electrooptical effect (Pockels effect).

S.I. Derzhavin, V.V. Kuz'minov, D.A. Mashkovskii, V.N. Timoshkin A.M. Prokhorov General Physics Institute, Russian Academy of Sciences, ul. Vavilova 38, 119991 Moscow, Russia; e-mail: derzh@kapella.gpi.ru

Received 8 December 2006; revision received 6 February 2007
Kvantovaya Elektronika **37** (7) 639 – 644 (2007)
Translated by M.N. Sapozhnikov

This crystal satisfies all the requirements listed above, except the fourth one. To fulfil this requirement, it is necessary to study specific physical and technical limitations appearing during operation of the modulator.

2. Parameters of the $LiNbO_3$ modulator

The optical axis of a $LiNbO_3$ crystal in our experimental scheme (Fig. 1) was oriented along a modulated laser beam (along the z axis), the laser radiation being linearly polarised along the y axis. The electric voltage producing the transverse electrooptical effect was applied to the $LiNbO_3$ crystal faces normal to the x axis. The required operation voltage was determined from the expression

$$V = \frac{d}{2L} V_{\lambda/2}, \quad V_{\lambda/2} = \frac{\lambda}{2n_o^3 r_{22}}, \tag{2}$$

where $V_{\lambda/2}$ is the half-wave voltage; d is the crystal thickness; $n_o = 2.29$; and r_{22} is the electrooptical coefficient equal to 3.4×10^{-10} cm V^{-1} for $LiNbO_3$.

Analysis of expression (2) shows that, by selecting properly the ratio L/d, the voltage applied to the crystal can be considerably reduced. For example, for $L = 10$ mm and $d = 0.5$ mm, we have $V \sim 250$ V.

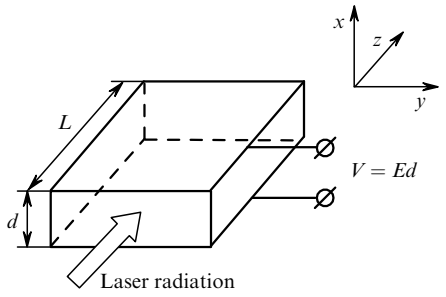

Figure 1. Transverse light modulator.

3. Restrictions in the modulator operation

In designing multichannel electrooptical modulators it is necessary to take into account the factors affecting the transmission and contrast of the modulator. These factors include the diffraction of radiation, crosstalk between channels, optically induced birefringence (photorefractive effect) [1] observed in the case of high radiation densities, and the secondary electrooptical effect [2].

3.1 Diffraction restrictions

The destructive role of radiation diffraction is manifested in a decrease in the modulation depth due to the additional (with respect to the parallel beam) phase incursion in the beam of nonparallel rays. This restricts the admissible divergence angle of the input beam, which is a serious disadvantage in most cases.

It is known that the expression for the crystal birefringence in the paraxial approximation has the form [3]

$$\Delta n \approx \frac{n_o^2}{2}\left(\frac{1}{n_e^2} - \frac{1}{n_o^2}\right)\varphi^2, \tag{3}$$

where φ is the angle of deviation of the light beam from the optical axis. The transparency T of a modulator in a system of crossed polarisers for linearly polarised radiation incident on the crystal is described by the expression [2]

$$T = \frac{\langle E_{in}^2 \rangle}{\langle E_{out}^2 \rangle} = \sin^2 2\beta \sin^2\left[\frac{\pi L}{\lambda}\frac{n_o^3}{2}\left(\frac{1}{n_e^2} - \frac{1}{n_o^2}\right)\varphi^2\right], \tag{4}$$

where $\langle E_{in}^2 \rangle$ and $\langle E_{out}^2 \rangle$ are the squares of the field amplitudes averaged over the oscillation period at the input and output, respectively; and β is the azimuthal angle of incidence of the beam.

In the presence of an external modulating field, expressions (3) and (4) have different forms. However, as shown in [3], the angular aperture of the $LiNbO_3$ modulator elements in an external field and its absence is approximately the same and is described by the relation

$$T = \sin^2 2\beta \sin^2\left(\frac{\pi}{4} A_{\lambda/2}\right), \tag{5}$$

where the quantity

$$A_{\lambda/2} = \frac{2Ln_o^3\varphi^2}{\lambda}\left(\frac{1}{n_e^2} - \frac{1}{n_o^2}\right) \tag{6}$$

is the ratio of the phase difference caused by the beam deviation from the optical axis and the induced half-wave field. Thus, the increase in the angular aperture φ is achieved by using crystals with a weaker birefringence or by reducing the crystal length, which is not always possible. The angular aperture for the $LiNbO_3$ crystal ($n_o = 2.29$, $n_e = 2.20$) for $L = 10$ mm, $\lambda = 0.8$ μm, and the required modulation depth of 90 % is estimated from (3)–(6) to be a few mrad.

We determined the angle φ experimentally by using the setup shown schematically in Fig. 2. A light beam emerging from fibre (*1*) of diameter 200 μm was collimated by lens (*2*) and directed on Glan prism (*3*) (another element withstanding the incident radiation load can be also used) to obtain polarised radiation. Then, the beam was diaphragmed [the diameter of diaphragm (*4*) was 2 mm], focused by lens (*5*) on probe $LiNbO_3$ crystal (*6*) so that it had the waist diameter equal to 4 mm and a plane wavefront within the crystal. The polarisation of the beam propagated through the $LiNbO_3$ crystal was studied by analyser (*7*) and power meter (*8*). For the optical-system parameters used in the study estimated from (3)–(6), the radiation power P_{in} behind diaphragm (*4*) was 250 mW for the pump current $I = 13$ A.

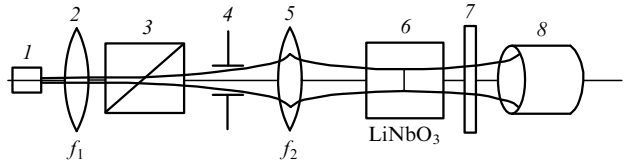

Figure 2. Optical scheme for measuring the modulator parameters: (*1*) radiation beam emerging from a fibre; (*2*) collimating lens; (*3*) Glan prism; (*4*) aperture; (*5*) focusing lens; (*6*) $LiNbO_3$ crystal; (*7*) analyser; (*8*) power meter; $f_1 = 1$ cm and $f_2 = 20$ cm are the focal distances of lenses (*2*) and (*5*), respectively.

Figure 3 presents the angular dependence of the modulator transmission. One can see that to provide the operation of the modulator, the angle φ should not exceed $\varphi_{max} \approx 1-2$ mrad. The geometry of a prototype sample was determined based on the angular restrictions and the beam-quality parameter $M^2 = 5$. For this purpose, it was necessary to establish the relation between the parameters L, d, φ, and V.

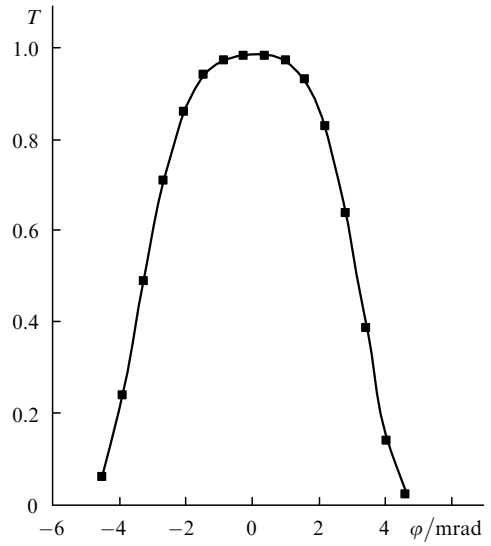

Figure 3. Angular dependence of the modulator transmission.

The width $w(z)$ of a beam (at the 1/e level in the field) in the Gaussian approximation is described by the expression

$$w^2(z) = w_0^2 + \left(\frac{M^2\lambda}{\pi w_0}\right) z^2,$$

where w_0 is the beam-waist radius and z is the beam coordinate along its propagation direction. Let us determine the local angle $\theta(z)$

$$\theta(z) = \frac{\mathrm{d}w(z)}{\mathrm{d}z} = \theta_{max} \frac{z}{(w_0^2 + \theta_{max} z^2)^{1/2}}, \qquad (7)$$

where

$$\theta_{max} = \frac{M^2\lambda}{\pi w_0}$$

is the far-field angle. Taking into account the angular restrictions pointed out above, we obtain

$$\theta(z) \leqslant \varphi_{max},$$
$$M^2 = \frac{\pi w_0 \theta_{max}}{\lambda} = 5. \qquad (8)$$

The length L and thickness d of the modulator are calculated from (7) taking (8) into account.

The parameters of the modulator were determined by using the following algorithm. Based on the properties of a 12-W cw HLU20F400 laser diode array with a fibre pigtail used in experiments, we modified the optical scheme to provide a radiation source with the required beam-quality parameter ($M^2 = 5$). The waist diameter was selected so that the radiation divergence over the waist length L =10 mm did not exceed $\varphi_{max} \approx 1$ mrad. In our case, this gave $w_0 \approx 0.15$ mm. The radiation power P_{in} incident on the modulator was 22 mW for the current $I = 20$ A. The obtained experimental values correspond to the values calculated by expression (7) under condition (8) taking into account the decrease in the waist diameter due to the propagation of light in a medium with the refractive index $n = 2.2$. Figure 4 shows the calculated dependence of the local angle θ on the coordinate z.

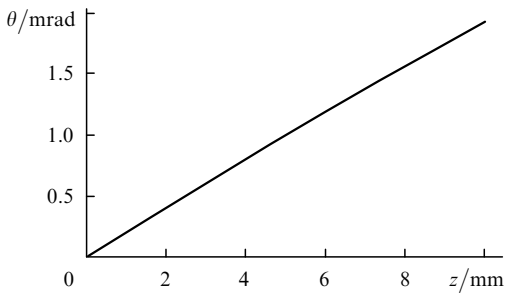

Figure 4. Dependence of the local angle θ on the coordinate z for $w_0 = 0.15$ mm and $M^2 = 5$.

Thus, for the waist diameter in the field $2w_0 = 0.3$ mm and the crystal dimensions $L = 10$ mm and $d = 2(w_0 + \delta) = 0.5$ mm (where δ is the empirical parameter), diffraction restrictions are satisfied.

Because the voltage V (2) can be decreased by increasing the modulator length L, the problem of optimisation appears because parameters L and d are interrelated. For this reason, we fabricated four prototype samples with different parameters which are presented in Table 1. To avoid the damage of the optical end faces of the modulator during the assembling of electrodes, the modulator length L_m exceeded the electrode length L_e by 1 mm in all samples.

Table 1. Restrictions caused by the channel crosstalk.

L_m/mm	L_e/mm	d/mm	V/V
11	10	0.5	265
11	10	0.6	280
16	15	0.8	290
16	15	1.0	360

Having measured the crystal length d, we find the width s of an electric contact. For this purpose, we studied experimentally the transmission of one channel of the modulator for different values of s. The optical scheme of the experiment is shown in Fig. 5.

Taking into account that, to obtain the efficient modulation of radiation, the electric field applied to the crystal should be uniform in the beam propagation region, we used the contact widths $s = 0.9$ and 0.6 mm for modulators of thickness $d = 0.5$ and 0.6 mm, respectively. Figure 6 shows the transmission of the modulator with $d = 0.5$ mm. The transmission curves presented in Fig. 6 give the optimal width of the contact $s = 0.6$ mm because in this case the transmission curve has no pronounced horizontal flat part at the top, as for $s = 0.9$ mm. This flat part determines the

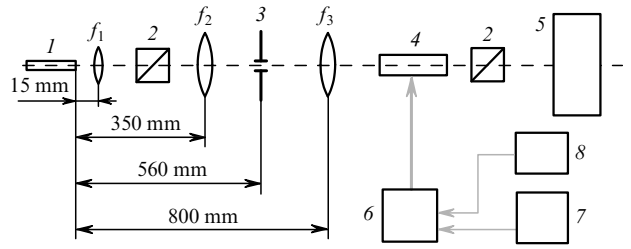

Figure 5. Optical scheme of the experimental setup: (*1*) HLU12F400-808 fibre output; (*2*) Glan prism; (*3*) aperture of diameter 0.5–1 mm; (*4*) modulator; (*5*) measurement instruments (power meter or a photodetector with an oscilloscope); (*6*) five-channel control unit; (*7*) generator of rectangular pulses of duration up to 10 μs with a pulse repletion rate up to 100 kHz and voltage 5 V; (*8*) dc voltage source (up to +500 V); $f_1 = 12$ mm; $f_2 = 250 - 320$ mm; $f_3 = 70$ mm.

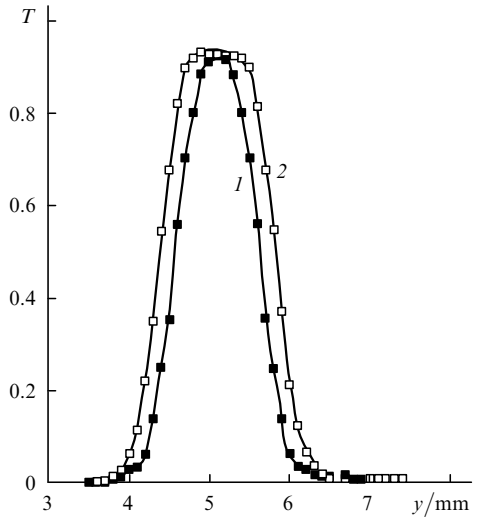

Figure 6. Modulator transmission for $s = 0.6$ (*1*) and 0.9 mm (*2*).

excess width of the electrode. The narrow maximum of the transmission curve for $s = 0.6$ mm suggests that the transmission of the channel will decrease with further decreasing the electrode width.

For the pump current of the diode $I = 15$ A, the radiation power incident on the crystal is $P_{in} = 30$ mW, the output power behind the modulator in the absence of the applied field ($V = 0$) is $P_{out} = 21.3$ mW, and in the presence of the field $V = 280$ V, the output power is 1.1 mW. As a result, we have the ratio $P_{out}(V = 0)/P_{out}(V = 280\ \text{V}) = 19.37$. For the current $I = 20$ A ($P_{in} = 52$ mW), this ratio is 18.1.

3.2 Mutual influence of channels

The layout of electrodes on the crystal faces (Fig. 7) should take into account the mutual influence of adjacent channels, which is manifested in the redistribution of control fields in the region of switched-on channels, the penetration of the fields of switched-on channels into the region of switched-off channels, as well as in the electrostatic induction of charges on adjacent electrodes. The latter circumstance, as experiments have shown, is insignificant because pairs of adjacent electrodes prove to be short-circuited through the output resistance of electron control units. The influence of the rest of the channels, except neighbouring ones, on an individual channel is rather weak, which is explained both by a rapid decrease of the field on the boundary of a flat capacitor and the screening action of the electrodes of adjacent channels. The redistribution of the fields leads to the nonuniform transmission of a completely open channel upon the commutation of adjacent channels, and their penetration to the adjacent channels reduces the modulator contrast, which also depends on the commutation of channels.

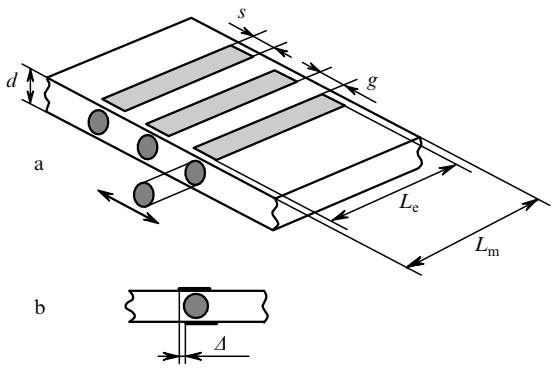

Figure 7. Scheme of the experiment for determining the required interelectrode gap.

To perform a series of experiments on measuring the minimal gap width g between electrodes on the modulator (Fig. 7), we fabricated samples with gaps $g = 1.2$, 1.1, 1.0, 0.9, and 0.8 mm. The negative electrodes were connected with a thin hook-up wire, which did not affect the modulator operation but simplified the application of the electric voltage by using one wire on the lower side of the modulator, which in turn could be located on a Teflon base rather than fixed only on side faces (Fig. 7). The electrode width s was 0.5 and 0.6 mm, and the modulator thickness was $d = 0.5$ mm.

We measured the dependence of the transmission of a laser beam on its displacement along the transverse coordinate with respect to the optical axis by switching alternatively two adjacent channels. The minimal gap width g, at which the influence of the adjacent channel on the channel under study is still absent, was measured to be 0.8 mm. This follows from the dependences presented in Fig. 8. Curves (*1*) and (*2*) correspond to the transmission in each of the channels when the adjacent channel is switched off. Straight lines (*3*) show the position of electrodes. One can see that when the laser beam passes through the point $y = 5.1$ mm for one channel and point $y = 6.6$ mm for another channel, the modulator has the maximal transmission. The same points are the centres of electrodes. But the most important is the fact that curves (*1*) and (*2*) have minima at points $y = 5.1$ and 6.6 mm, respectively, i.e. when the laser beam is located exactly under the electrode axial line, it will not be affected by the adjacent channel. Thus, the electrode gap for the 0.5-mm-thick modulator should be no less than 0.8 mm.

3.3 Photorefraction-induced restrictions

One of the peculiarities of the operation of modulators is a high radiation power density caused by a small linear aperture of the modulator and the relatively high radiation power required for technological processing. For 100 mW

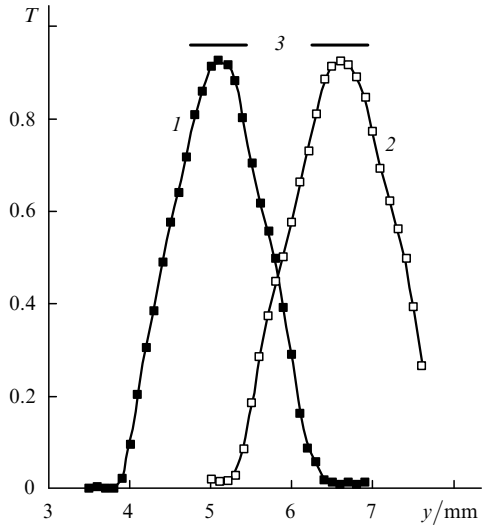

Figure 8. Transmission in two alternatively switched adjacent channels (*1*, *2*) as a function of the laser-beam displacement along the transverse coordinate y. Straight lines (*3*) are the positions of electrodes.

of the radiation power per channel, the power density can achieve 1 kW cm^{-2}.

Laser radiation of such high power densities can change birefringence due to photogeneration and subsequent capture of photoexcited electrons by traps. The redistribution of charges along the spontaneous polarisation axis caused by its process leads to a change in the crystal field, which is related to the refractive index through the electrooptical effect. The short-wavelength radiation strongly affects the photorefractive effect due to excitation of charge carriers from the deeper levels of the forbidden zone of the crystal [4]. Upon exposure of a $LiNbO_3$ crystal to the 488-nm radiation incident perpendicular to the optical axis, the effect is manifested for radiation power densities of a few W cm^{-2}. However, irradiation along the optical axis (as in our configuration) does not induce birefringence [5]. Upon irradiation at 532 nm, the photorefractive effect was not observed for power densities up to 10 MW cm^{-2}, while upon irradiation at 1064 nm this effect was not detected for power densities up to 5 kW cm^{-2}. We studied the photorefractive effect at a wavelength of 800 nm used in our problem.

The photorefractive effect was analysed by measuring the rotation of the polarisation axes of radiation transmitted through the modulator. The radiation of power $P_{in} = 3.8$ W was focused into a spot of diameter 0.3 mm on the modulator, which corresponds to the power density ~ 5 kW cm^{-2}. We have failed to detect any noticeable rotation of the polarisation ellipsis both in the presence and absence of voltage on the modulator contacts. Thus, this result allows us to neglect the destructive role of photorefraction for the required radiation power $P_{in} =$ 100 mW incident on the channel of a modulator of thickness $d = 0.5$ mm and more.

3.4 Restrictions caused by the secondary electrooptical effect

The potentially fast response of the electrooptical effect, determined by the polarisation time ($\sim 10^{-14}$ s), is restricted by the distortions of the amplitude–frequency characteristics of the modulator related to piezoelectric resonances. Due to the same symmetry of the electrooptical and piezoelectric effects, all media having one of these effects also possess necessarily the other. This means that an alternating electric field applied to an electrooptical crystal induces, along with the electron or lattice polarisation responsible for variations in optical properties, the elastic stress waves. When the control-voltage frequencies coincide with the frequencies of mechanical resonances in the crystal, which depend on its size and elastic properties, standing waves are produced, i.e. a piezoelectric resonance appears. In this case, elastic stresses change the optical parameters of the electrooptical crystal due to the elastooptical effect, which can be treated as the additional contribution to the electrooptical effect, which is called the secondary electrooptical effect. As a result, the amplitude–frequency characteristics of the crystal are distorted. These distortions cannot be corrected by radio engineering methods because the spectrum of resonance frequencies is rather broad, while the Q factor of such resonators exceeds tens of thousands.

According to the type of excitation of elastic waves, electrooptical elements are the resonance structures, which are well studied [1]. It is shown that the first resonances are observed in them at the control action frequencies $f_k = vk/(2d)$, where v is the sound speed in the medium and k is the harmonic number.

Because the analytic description of piezoelectric excitation of an electrooptical element is complicated, especially in the case of the inhomogeneous distribution of the control fields in multichannel light modulators, this process is described empirically. In addition, a great number of simultaneously operating channels and their arbitrary commutation additionally enrich the frequency spectrum. Taking this into account, all the resonance frequencies can be conventionally divided into two groups: the resonance frequencies whose formation can be considered by neglecting reflections from the side faces of the element, and the resonance frequencies that are formed due to reflections from the side faces of the element. It is obvious that frequencies in first group are higher. The frequencies of the first resonances in this group depend on the element thickness and lie between 2 and 4 MHz for thicknesses between 0.5 and 1 mm. This frequency range determines the transmission bandwidth of the modulator.

It follows from the above estimates that in the case of low frequencies (no more than 100 kHz) and resonator thicknesses (no less than 0.5 mm), no piezoelectric effect should be observed. However, the duration ~ 200 ns of the leading edge of pulses used in experiments can cause the piezoelectric effect.

Our experimental studies of a 0.5-mm-thick unfastened modulator showed the presence of electric oscillation resonances at frequencies about 100 kHz at a voltage of 320 V applied to the crystal. They were revealed in the form of a slight (~ 6 %) modulation of the tops of voltage pulse amplitudes. When the modulator was fixed in the base with an elastic compound, the resonances disappeared completely up to voltages 500 V and pulse repetition rate up to 120 kHz. Note that we did not use any additional coverings of the modulator. This voltage modulation was not detected for optical pulses.

The piezoelectric effect also causes the modulator heating. The modulator temperature was controlled in experiments with an accuracy of $\pm 2\,^{\circ}$C by using a TV camera. No temperature variations were observed within

this inaccuracy. This result suggests indirectly that the piezoelectric effect is absent.

4. Electric scheme of the modulator

The power supply of the modulator consists of transistor switches for each channel and a five-channel master oscillator. The frequency and parameters of electric pulses are determined by an external generator separately for each channel. The control voltage depends on the modulator parameters, but should not exceed +500 V. One channel of the modulator requires a power supply providing a current of 50 mA and voltage up to +500 V.

The required pulse front duration (shorter than 1 μs) and stable modulator operation at high frequencies (up to 100 kHz) were provided by using a switch circuit with two IRF 830 field transistors and an IR 2104 standard driver recommended by International Rectifier. Such circuits were assembled for each of the five channels and were fed from one high-voltage source. To reduce the possible influence of the piezoelectric effect, the switch scheme provided the pulse rise and decay duration no less than 200 ns.

The final version of the prototype of a five-channel modulator is shown schematically in Fig. 7a. The modulator width was $d = 0.5 \pm 0.02$ mm, the electrode width $s = 0.6 \pm 0.005$ mm, the interelectrode distance $g = 0.8 \pm 0.01$ mm, the electrode length $L_e = 10$ mm, the modulator length $L_m = 11$ mm, the positioning errors for the upper and lower electrodes $\Delta = \pm 0.025$ mm (Fig. 7b), the non-parallelism of electrodes was no more than six angular minutes. The positioning errors obtained in the study provided the radiation modulation depth of 92 % for 52 mW of radiation incident on a channel and the beam quality parameter $M^2 = 5$.

5. Conclusions

Thus, we have fabricated the prototype of a five-channel $LiNbO_3$ electrooptical modulator. The modulator is intended for the modulation of the 0.8-μm cw radiation with power per channel up to 100 mW. The modulation frequency does not exceed 100 kHz and the modulation depth is 92 %.

Acknowledgements. The authors thank L.B. Arkhontov for his attention to our work. This work was supported by the LIMO company (Germany).

References

1. Mustel E.R., Parygin V.N. *Metody modulyatsii i skanirovaniya sveta* (Methods for Light Modulation and Scan) (Moscow: Nauka, 1970).
2. Sirotin Yu.I., Shaskol'skaya M.P. *Osnovy kristallofiziki* (Fundamentals of Crystal Physics) (Mocow: Nauka, 1979).
3. Arkhontov L.B., Geras'kin V.V., Kiselev B.S. *Kristallografia*, **27**, 528 (1982).
4. Chen P.S. *J. Appl. Phys.*, **40**, 3389 (1969).
5. Smakula P.H., Claspy P.C. *Trans. Met. Soc. AIME*, **239**, 421 (1967).